1994

Polynomial Surface Patch Representations

Chandrajit L. Bajaj

Report Number:

94-038

Polynomial Surface Patch Representations

Chandrajit L. Bajaj
Computer Sciences Department
Purdue University
West Lafayette, IN 47907

CSD-TR-94-038
May, 1994

SIGGRAPH 94 COURSE NOTES
Polynomial Surface Patch Representations

Chandrajit L. Bajaj*
Department of Computer Science,
Purdue University,
West Lafayette, Indiana 47907

Email: bajaj@cs.purdue.edu

WWW/Xmosaic:: http://www.cs.purdue.edu/people/bajaj

Tel: 317-494-6531

Fax: 317-494-0739

May 11, 1994

1 INTRODUCTION

Our approach to the design and analysis of geometric algorithms for operations on polynomial (algebraic) curves and surfaces is to take the view of abstract data types, that is, a data representation coupled together with the operations on them [7, 8]. In this framework, the choice of which representation of the polynomial curve or surface patch to use is determined by the desired optimality of the geometric algorithms for the operations.

Polynomial curves and surfaces can be represented in an implicit form, and sometimes also in a parametric form. The implicit form of a real polynomial surface in $\mathbb{R}^3$ is

$$f(x, y, z) = 0 \tag{1}$$

where f is a polynomial with coefficients in $\mathbb{R}$. The parametric form, when it exists, for a real polynomial surface in $\mathbb{R}^3$ is

$$\begin{aligned} x &= \frac{f_1(s,t)}{f_4(s,t)} \\ y &= \frac{f_2(s,t)}{f_4(s,t)} \\ z &= \frac{f_3(s,t)}{f_4(s,t)} \end{aligned} \tag{2}$$

where the f_i are again polynomials with coefficients in $\mathbb{R}$. The above implicit form describes a two dimensional real algebraic variety (a surface) with a single polynomial equation in $\mathbb{R}^3$. The parametric form also describes a

*Supported in part by NSF grants CCR 92-22467, DMS 91-01424, AFOSR grants F49620-93-10138, F49620-94-1-0080, ONR grant N00014-94-1-0370 and NASA grant NAG-93-1-1473.

real two dimensional algebraic variety (a surface), however with a set of three independent polynomial equations in $\mathbb{R}^5$, with coordinate variables x, y, z, s, t. Alternatively, the parametric form of a real surface may also be interpreted as a rational mapping from $\mathbb{R}^2$ to $\mathbb{R}^3$. We can thus compare the implicit and parametric representations of polynomial surfaces by considering the the parametric form either as a *mapping* or alternatively, an *algebraic variety*.

In these notes, we consider specific geometric operations of display/finite element mesh generation and data fitting, and compare the implicit and parametric polynomial forms for their superiority (or lack thereof) in optimizing algorithms for operations in these categories.

Section 2 sets the terminology and introduces some well known facts about polynomial curves and surfaces and their patch representations. Section 3 compares the implicit and parametric surface representations for graphics display and triangular mesh generation operations. Here the rational mapping gives an advantage to the parametric form, though the algorithms to solve this problem in this representation are still non-trivial. Section 4 considers the tradeoff between implicit and parametric surface splines for interactive design and data fitting operations.

2 PRELIMINARIES

2.1 Mathematical Terminology

In this section we review some basic terminology from algebraic geometry that we shall use in subsequent sections. These and additional facts can be found for example in [64, 68].

The set of real and complex solutions (or *zero* set $Z(C)$) of a collection C of polynomial equations

$$\begin{aligned} f_1(x_1, ..., x_d) &= 0 \\ &\vdots \\ f_m(x_1, ..., x_d) &= 0 \end{aligned} \tag{3}$$

with coefficients over the reals $\mathbb{R}$ or complexes $\mathbb{C}$, is referred to as an *algebraic set*. The algebraic set defined by a single equation ($m = 1$) is also known as a hypersurface. A algebraic set that cannot be represented as the union of two other distinct algebraic sets, neither containing the other, is said to be *irreducible*. An irreducible algebraic set $Z(C)$ is also known as an *algebraic variety* V.

A hypersurface in $\mathbb{R}^d$, some d dimensional space, is of *dimension* $d-1$. The *dimension* of an algebraic variety V is k if its points can be put in (1,1) rational correspondence with the points of an irreducible hypersurface in $k+1$ dimensional space. In $\mathbb{R}^d$, a variety V_1 of dimension k intersects a a variety V_2 of dimension h, with $h \geq d-k$, in an algebraic set $Z(S)$ of dimension at least $h+k-d$. The resulting intersection is termed *proper* if all subvarieties of $Z(S)$ are of the same minimum dimension $h+k-n$. Otherwise the intersection is termed *excess* or *improper*. Let the *algebraic degree* of an algebraic variety V be the *maximum* degree of any defining polynomial. A degree 1 hypersurface is also called a *hyperplane* while a degree 1 algebraic variety of dimension k is also called a *k-flat*. The *geometric degree* of a variety V of dimension k in some $\mathbb{R}^d$ is the maximum number of intersections between V and a $(d-k)$-flat, counting both real and complex intersections and intersections at infinity. Hence the geometric degree of an algebraic hypersurface is the maximum number of intersections between the hypersurface and a line, counting both real and complex intersections and at infinity.

The following theorem, perhaps the oldest in algebraic geometry, summarizes the resulting geometric degree of intersections of varieties of different degrees.

[Bezout] A variety of geometric degree p which *properly* intersects a variety of geometric degree q does so in an algebraic set of geometric degree either at most pq or infinity. $\diamond$

The *normal* or *gradient* of a hypersurface $\mathcal{H} : f(x_1, ..., x_n) = 0$ is the vector $\nabla f = (f_{x_1}, f_{x_2}, \ldots, f_{x_n})$. A point $\mathbf{p} = (a_0, a_1, \ldots a_n)$ on a hypersurface is a *regular* point if the gradient at $\mathbf{p}$ is not null; otherwise the point is *singular*. A singular point $\mathbf{q}$ is of multiplicity e for a hypersurface $\mathcal{H}$ of degree d if any line through $\mathbf{q}$ meets $\mathcal{H}$ in at most $d-e$ additional points. Similarly a singular point $\mathbf{q}$ is of multiplicity e for a variety V in $\mathbb{R}^n$ of

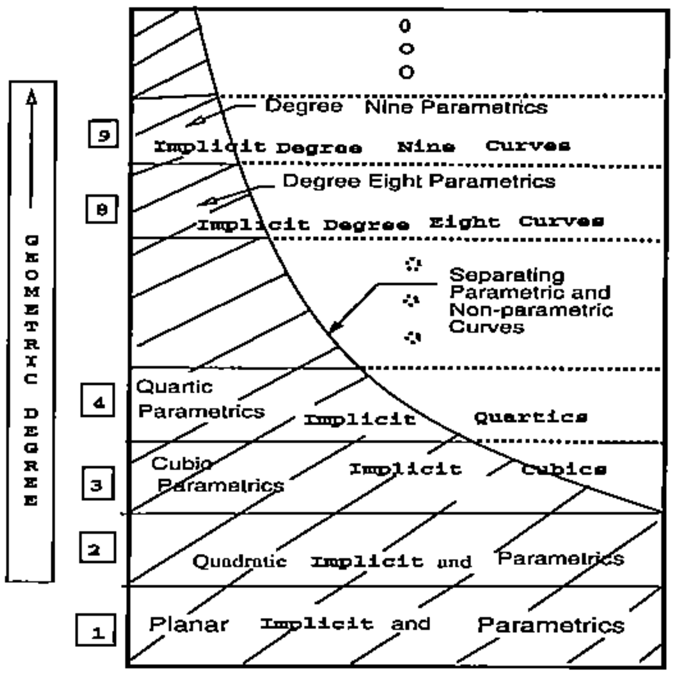

Figure 1: A Classification of Low Degree Algebraic Curves

dimension k and degree d if any sub-space $\mathbb{R}^{n-k}$ through q meets V in at most $d - e$ additional points. It is important to note that even if two varieties intersect in a *proper* manner, their intersection in general may consist of sub-varieties of various multiplicites. The total degree of the intersection, however is bounded by Bezout's theorem. Finally, one notes that a hypersurface $f(x_1, ..., x_n) = 0$ of degree d has $K = \binom{n+d}{n}$ coefficients, which is one more than the number of independent coefficients. Hypersurfaces $f(x_1, ..., x_n) = 0$ of degree d form $K - 1$ dimensional vector spaces over the field of coefficients of the polynomials.

Finally, two hypersurfaces $f(x_1, \ldots, x_n) = 0$ and $g(x_1, \ldots, x_n) = 0$ meet with C^k-continuity along a common subvariety V if and only if there exist functions $\alpha(x_1, \ldots, x_n)$ and $\beta(x_1, \ldots, x_n)$ such that all derivatives upto order k of $\alpha f - \beta g$ equals zero at all points along V, see for e.g., [36].

2.2 Polynomial Curves and Surfaces

We cast our real implicit and parametric curves and surfaces, in the terminology of the previous subsection. A real implicit algebraic plane curve $f(x, y) = 0$ is a hypersurface of dimension 1 in $\mathbb{R}^2$, while a parametric plane curve $[f_3(s)x - f_1(s) = 0, f_3(s)y - f_2(s) = 0]$ is an algebraic variety of dimension 1 in $\mathbb{R}^3$, defined by the two independent algebraic equations in the three variables x, y, s. Similarly, a real implicit algebraic surface $f(x, y, z) = 0$ is a hypersurface of dimension 2 in $\mathbb{R}^3$, while a parametric surface $[f_4(s, t)x - f_1(s, t) = 0, f_4(s, t)y - f_2(s, t) = 0, f_4(s, t)z - f_3(s, t) = 0]$ is an algebraic variety of dimension 2 in $\mathbb{R}^5$, defined by three independent algebraic equations in the five variables x, y, z, s, t.

A plane parametric curve is a very special algebraic variety of dimension 1 in x, y, s space, since the curve lies in the 2-dimensional subspace defined by x, y and furthermore points on the curve can be put in $(1, 1)$ rational correspondence with points on the 1-dimensional sub-space defined by s. Parametric curves are thus a special subset of algebraic curves, and are often also called rational algebraic curves. Figure 1 depicts the relationship between the set of parametric curves and non-parametric curves at various degrees.

Example parametric (rational algebraic) curves are degree two algebraic curves (conics) and degree three algebraic curves (cubics) with a singular point. The non-singular cubics are not rational and are also known

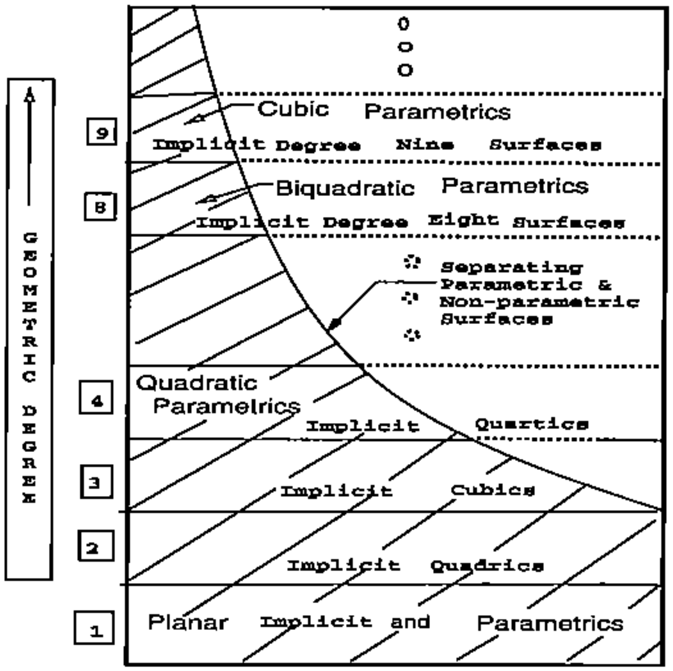

Figure 2: A Classification of Low Degree Algebraic Surfaces

as elliptic cubics. In general, a necessary and sufficient condition for the rationality of an algebraic curve of arbitrary degree is given by the Cayley-Riemann criterion: a curve is rational iff $g = 0$, where g, the genus of the curve is a measure of the deficiency of the curve's singularities from its maximum allowable limit [66]. Algorithms for computing the genus of an algebraic curve and for symbolically deriving the parametric equations of genus 0 curves, are given for example in [1, 2, 3].

Similarly, a parametric surface is a very special algebraic variety of dimension 2 in x, y, z, s, t space, since the surface lies in the 3-dimensional subspace defined by x, y, z and furthermore points on the surface can be put in $(1,1)$ rational correspondence with points on the 2-dimensional sub-space defined by s, t. Figure 2 depicts the relationship between parametric and non-parametric surfaces.

Example parametric (rational algebraic) surfaces are degree two algebraic surfaces (quadrics) and most degree three algebraic surfaces (cubic surfaces). The cylinders of nonsingular cubic curves and the cubic surface cone are of not rational. Other examples of rational algebraic surfaces are Steiner surfaces which are degree four surfaces with a triple point, and Plücker surfaces which are degree four surfaces with a double curve. In general, a necessary and sufficient condition for the rationality of an algebraic surface of arbitrary degree is given by Castelnuovo's criterion: $P_a = P_2 = 0$, where P_a is the arithmetic genus and P_2 is the second plurigenus [67]. Algorithms for symbolically deriving the parametric equations of degree two and three rational surfaces are given in [1, 2, 3, 4, 62].

2.3 Degree & Singularities

For implicit algebraic plane curves and surfaces defined by polynomials of degree d, the maximum number of intersections between the curve and a line in the plane or the surface and a line in space, is equal to the maximum number of roots of a polynomial of degree d. Hence, here the geometric degree is the same as the algebraic degree which is equal to d. For parametric curves defined by polynomials of degree d, the maximum number of intersections between the curve and a line in the plane is also equal to the maximum number of roots of a polynomial of degree d. Hence here again the geometric degree is the same as the algebraic degree. For parametric surfaces defined by polynomials of degree d the geometric degree can be as large as d^2, the square of the algebraic degree d. This can be seen as follows. Consider the intersection of a generic line in space $[a_1x + b_1y + c_1z - d_1 = 0, a_2x + b_2y + c_2z - d_2 = 0]$ with the parametric surface. The intersection yields two implicit algebraic curves of degree d which intersect in $O(d^2)$ points (via Bezout's theorem), corresponding to the intersection points of the line and the parametric surface.

A parametric curve of algebraic degree d is an algebraic curve of genus 0 and so have $\frac{(d-1)(d-2)}{2} = O(d^2)$ singular (double) points. This number is the maximum number of singular points an algebraic curve of degree d may have. From Bezout's theorem, we realize that the intersection of two implicit surfaces of algebraic degree d can be a curve of geometric degree $O(d^2)$. Furthermore the same theorem implies that the intersection of two parametric surfaces of algebraic degree d (and geometric degree $O(d^2)$) can be a curve of geometric degree $O(d^4)$. Hence, while the potential singularities of the space curve defined by the intersection of two implicit surfaces defined by polynomials of degree d can be as many as $O(d^4)$, the potential singularities of the space curve defined by the intersection of two parametric surfaces defined by polynomials of degree d can be as many as $O(d^8)$.

2.4 Polynomial Patch Representations

The popular polynomial bases amongst interactive geometric designers are the Bernstein-Bézier and the B-Spline basis. These bases are defined for restricted subdomains of the deining space as opposed to the power basis which is defined for all points of the space. The example formulations given below are defined for values of each of the variables x, y and z in the unit interval [0,1].

Bernstein-Bézier Basis (BB)

Univariate:

$$P(x) = \sum_{j=0}^{m} w_j B_j^m(x)$$

where

$$B_i^m(x) = \binom{m}{i} x^i (1-x)^{m-i}$$

Bivariate:

(1) Tensor:

$$P(x,y) = \sum_{i=0}^{m}\sum_{j=0}^{n} w_{ij} B_i^n(x) B_j^n(y)$$

(2) Barycentric:

$$P(x,y) = \sum_{i=0}^{m}\sum_{j=0}^{m-i} w_{ij} B_{ij}^n(x,y)$$

where

$$B_{ij}^m(x,y) = \binom{m}{ij} x^i y^j (1-x-y)^{m-i-j}$$

Trivariate:

(1) Tensor:

$$P(x,y,z) = \sum_{i=0}^{m}\sum_{j=0}^{n}\sum_{k=0}^{p} w_{ijk} B_i^n(x) B_j^n(y) B_k^n(z)$$

(2) Mixed:

$$P(x,y,z) = \sum_{i=0}^{m}\sum_{j=0}^{m-i}\sum_{k=0}^{p} \mathrm{b}_{ijk} B_{ij}^n(x,y) B_k^n(z)$$

(3) Barycentric:

$$P(x,y,z) = \sum_{i=0}^{m} \sum_{j=0}^{m-i} \sum_{k=0}^{m-i-j} w_{ijk} B_{ijk}^{m}(x,y,z)$$

where

$$B_{ijk}^{m}(x,y,z) = \binom{m}{ijk} x^i y^j z^k (1-x-y-z)^{m-i-j-k}$$

The B-spline basis over the unit interval [0,1] is easily generated by a fractional linear recurrence as given below for the univariate case. The bivariate and trivariate forms can also be similarly generated from this in either tensor product or barycentric form, as given for the BB form above.

B-Spline Basis
Univariate:

$$\mathbf{P}_n = \sum_{l=0}^{m} \mathbf{p}_l N_l^n(x)$$

where

$$N_l^1(x) = \begin{cases} 1 \text{ for } x_l \le x_{l+1} \\ 0 \text{ otherwise.} \end{cases}$$

and knot sequence $0 = u_0 \le u_1 < \ldots < u_{m+1} = 1$

$$N_l^n(x) = \frac{x - x_{l-1}}{x_{l+n-1} - x_{l-1}} N_l^{n-1}(x) + \frac{x_{l+n} - x}{x_{l+n} - x_l} N_{l+1}^{n-1}(x)$$

Both the parametric and the implicit representation of algebraic curve segments and algebraic surface patches can be represented in either of the above BB or B-spline bases. Note that the canonical representation of a parametric plane curve segment and surface patch in x, y, z space are given by Curve:

$$\begin{cases} x = P_1(t), \\ y = P_2(t), \\ w = P_3(t). \end{cases}$$

Surface:

$$\begin{cases} x = P_1(s,t), \\ y = P_2(s,t), \\ z = P_3(s,t), \\ w = P_4(s,t). \end{cases}$$

where the P_i are polynomials in any of the above appropriate bases and the variables/parameters s, and t range over the unit interval [0,1].

An implicit curve segment and surface patch can be defined in x, y, z space by Curve:

$$z = P(x,y) \wedge z = 0$$

Surface:

$$w = P(x,y,z) \wedge w = 0$$

where the P is a polynomial in any of the above appropriate basis and the variables x, y, z range over the unit interval [0,1].

The work of characterizing the BB form of polynomials within a tetrahedron such that the zero contour of the polynomial is a single sheeted surface within the tetrahedron, has been attempted in the past. In [60], Sederberg showed that if the coefficients of the BB form of the trivariate polynomial on the lines that parallel one edge, say L, of the tetrahedron, all increase (or decrease) monotonically in the same direction, then any line parallel to L will intersect the zero contour algebraic surface patch at most once. In [39], Guo treats the same problem by enforcing monotonicity conditions on a cubic polynomial along the direction from one vertex to a point of the

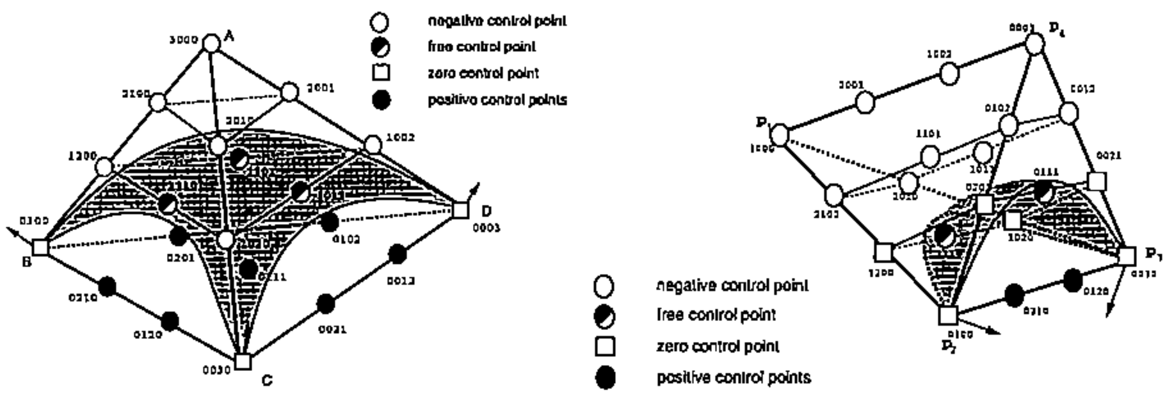

(a) (b)

Figure 3: (a) A three sided patch tangent at B, C, D (b) A degenerate four sided patch tangent to face $[p_1 p_2 p_4]$ at p_2 and $[p_1 p_3 p_4]$ at p_3

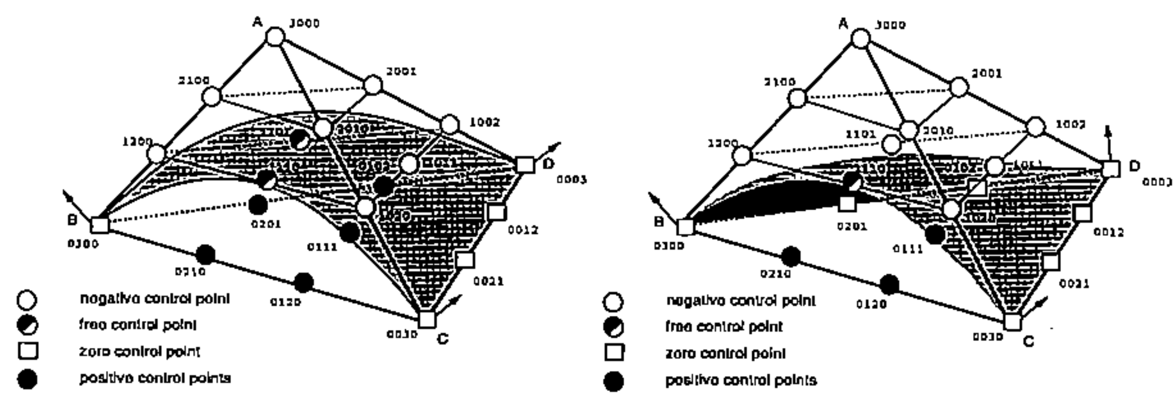

(a) (b)

Figure 4: (a) A three sided patch interpolating the edge CD (b) A three sided patch interpolating edges BD and CD

opposite face of the vertex. From this he derives a condition $a_{\lambda - e_1 + e_4} - a_\lambda \geq 0$ for all $\lambda = (\lambda_1, \lambda_2, \lambda_3, \lambda_4)^T$ with $\lambda_1 \geq 1$, where a_λ are the coefficients of the cubic in BB form and e_i is the i-*th* unit vector. This condition is difficult to satisfy in general, and even if this condition is satisfied, one still cannot avoid singularities on the zero contour. In[11, 10] sufficient conditions of a smooth, single sheeted zero contour generalizes Sederberg's condition and provides with an efficient way of generating nice implicit surface patches in BB-form (called A-patches for algebraic patches). See Figures 3 and 4.

3 DISPLAY & MESH GENERATION

We present two algorithms for computing planar triangular approximations (triangulations) of real algebraic surfaces, one specialized to the implicit representation[20], and the other for the rational parametric[16]. These are easily adaptable to different implicit and parametric surface patch representations. Modern day computer graphics hardware accept such triangulations and accurately render the complicated surfaces with sophisticated lighting and shading models. Similar planar triangular meshes of surfaces are required for finite element methods of solving systems of partial differential equations. See also [17, 19, 20, 21] for higher order, curved finite element approximations of implicit polynomial curves and surfaces with piecewise parametric splines.

3.0.1 Implicit Surfaces

To compute real points on implicit polynomial surfaces requires the solution of polynomial equations. Furthermore, the problem of constructing a polygonal approximation, especially for finite element meshes, is complicated by the need for a correct topology of the mesh even in the presence of singularities and multiple sheets of the real polynomial surface. Direct schemes which work for arbitrary implicit polynomial surfaces are based on the entire enclosing space: either the regular subdivision of the cube [23], a finite subdivision of an enclosing simplex [43], uniform refinement [49] or enclosing simplicial continuation [6] or enclosing cube continuation [25]. However, such spatial sampling methods fail in the presence of point and curve singularities of the polynomial surface, or yield ambiguous topologies in neighborhoods where multiple sheets of the surface come close together. Symbolic methods are necessary to disambiguate or calculate the correct topology for general polynomial curves and surfaces.

Our algorithm uses a triangular surface patch expansion scheme and works directly on the surface instead of a spatial subdivision. It requires a seed point for each real component of the polynomial surface. Compared to the above approaches the patch expansion is centered on points on the surface, and fully uses the polynomial and its derivatives to construct local neighborhoods of convergence. The point selection and hence the final triangulation is adaptive to the k^th order of derivatives (e.g. $k = 2$ implies curvature adaptive) selected for each expansion. By its very nature the triangulation generalizes to arbitrary analytic function surfaces and not just algebraic (polynomial) surfaces.

We begin with a few notational definitions

Expansible edge. During the process of expansion of the triangular mesh, an edge is called expansible if we can go further from this edge to obtain a new triangle on the surface. That is

(a) this edge is on the boundary of the presently constructed mesh

(b) this edge is inside the given boundary box.

The directional expansion, expansion point and the T-plane.

Let $p_0 = (p_0^x, p_0^y, p_0^z)$ be a point on the surface $f(x, y, z) = 0$. If

$$\left|\frac{\partial f(p_0)}{\partial z}\right| \qquad \left(\text{or } \left|\frac{\partial f(p_0)}{\partial x}\right|, \left|\frac{\partial f(p_0)}{\partial y}\right|\right) = ||\nabla f(p_0)||_\infty$$

then the surface $f(x, y, z) = 0$ can be expressed locally as a power (Taylor) series $z = \phi(x, y)$ (or $x = \phi(y, z)$, $y = \phi(x, z)$). We call this a *z-direction expansion*. The point p_0 is referred to as the *expansion point*. The

$\frac{\partial f(p_0)}{\partial x}(x - p_o^x) + \frac{\partial f(p_0)}{\partial y}(y - p_o^y) + \frac{\partial f(p_0)}{\partial z}(z - p_o^z) = 0$ the tangent plane of $f = 0$ at p_0, denoted by T-plane. The projection of a space point p onto the T-plane is denoted by $T(p)$.

The following algorithm constructs a triangular mesh on each real component of a real polynomial surface, within a given bounding box. We assume that we have a starting seed point on each real component of the surface in this bounded region. Several numeric and symbolic methods exist to compute such seed points [20, 28]

1. *Initial Step*: For a given seed point p_0 on a real component of the surface $f(x, y, z) = 0$, we first compute a directional expansion, say $z = \phi(x, y)$. On the T-plane, find a circle with center p_0 such that $\phi(x, y)$ is convergent within the circle. The computation of the radius of convergence, based on the k coefficient terms of a power series expansion are well known and given for example in [44]. Take three points on the circle uniformly, say q_0, q_1, q_2, and refine the points $(q_i, z(q_i))$ by a Newton iteration such that the resulting points V_i are on the surface. The triangle $[V_0, V_1, V_2]$ is the first one we want. Each edge of this triangle is expansible except perhaps if the seed point was chosen such that one edge is on the boundary of the surface with respect to the bounding box.

2. *General Step*: Suppose we have constructed several space triangles that form a connected mesh. Assume at least one edge (V_i, V_j) of a boundary triangle $[V_i, V_j, V_k]$ is expansible. Then the general step is to construct one or more triangles that connects to the edge (V_i, V_j)

   (a) Start from the expansion point P_{ijk} of the triangle $[V_i, V_j, V_k]$ and directional expansion, say $z = \phi(x, y)$. Choose one point Q on the T-plane at P_{ijk} within the convergence radius, such that Q is on the middle-perpendicular line of $[T(V_i), T(V_j)]$ and as far as possible from $T(P_{ijk})$.

   (b) Refine the point $(Q, z(Q))$ to a point on the surface, say Q_1. The point Q_1 becomes a new expansion point. Compute directional expansion at Q_1, say $z = \phi_1(x, y)$, and its circle of convergence. The triangulation around Q_1 is reconstructed as follows.

   - Let $[V_i, V_l]$ and $[V_j, V_m]$ be the neighboring edges of $[V_i, V_j]$. Then on the T-plane at point Q_1, if the angle $< T(V_j)T(V_i)T(V_l) \geq \frac{\pi}{2}$ and $< T(V_i)T(V_j)T(V_m) \geq \frac{\pi}{2}$ or the convergence circle has no intersection points with $[T(V_i), T(V_l)]$ and $[T(V_j), T(V_m)]$, then choose the intersection point Q_2 of the circle and the perpendicular line of $[T(V_i), T(V_j)]$ passing through $T(Q_1)$. If $(T(Q_1), Q_2)$ intersects a previous edge or the bounding box, then Q_2 is chosen to be this intersection point. Refine $(Q_2, \phi_1(Q_2))$ and obtain a new vertex V_n and form the new triangle $[V_i, V_j, V_n]$. Also see top part of Figure 5.
   - If the angle $< T(V_j)T(V_i)T(V_l) < \frac{\pi}{2}$ and $(T(V_i), T(V_j))$ intersect the circle (or, angle $< T(V_i)T(V_j)T(V_m) < \frac{\pi}{2}$ and $(T(V_j), T(V_m))$ intersects the circle), (see middle part of Figure 5, then take Q_1 as this intersection point. Otherwise take $Q_1 = T(V_l)$. In the first case, we add a point on the edge $[V_i, V_l]$ and divide it into two edges, $[V_i, V_l]$ and $[V_5, V_4]$. The $[V_2, V_4]$ is expansible and $[V_2, V_5]$ is not. A new expansible edge $[V_1, V_5]$ is produced. In the second case, edge $[V_i, V_j]$ and $[V_i, V_l]$ become non-expansible and a new expansible edge $[V_j, V_l]$ is generated. A related case is shown in the bottom part of Figure 5 and is handled in much the same fashion.

3. *Final Step*. We iterate the General Step, until every edge is non-expansible for that real component.

Figure 6 shows the triangulation of implicitly defined polynomial surfaces.

3.0.2 Rational Parametric Surfaces

A well-known strength of the parametric representation (its mapping from $\mathbb{R}^2$ to $\mathbb{R}^3$) is the ease by which real points can be generated on the parametric curve or surface. However the problem of constructing triangulations with consistent topology is still highly non-trivial. Arbitrary rational parametric surfaces have real *pole curves* in their domain, where the denominators of the parameter functions vanish, domain real *base points* for which all four numerator and denominator polynomials vanish simultaneously, and other features that cause naiive

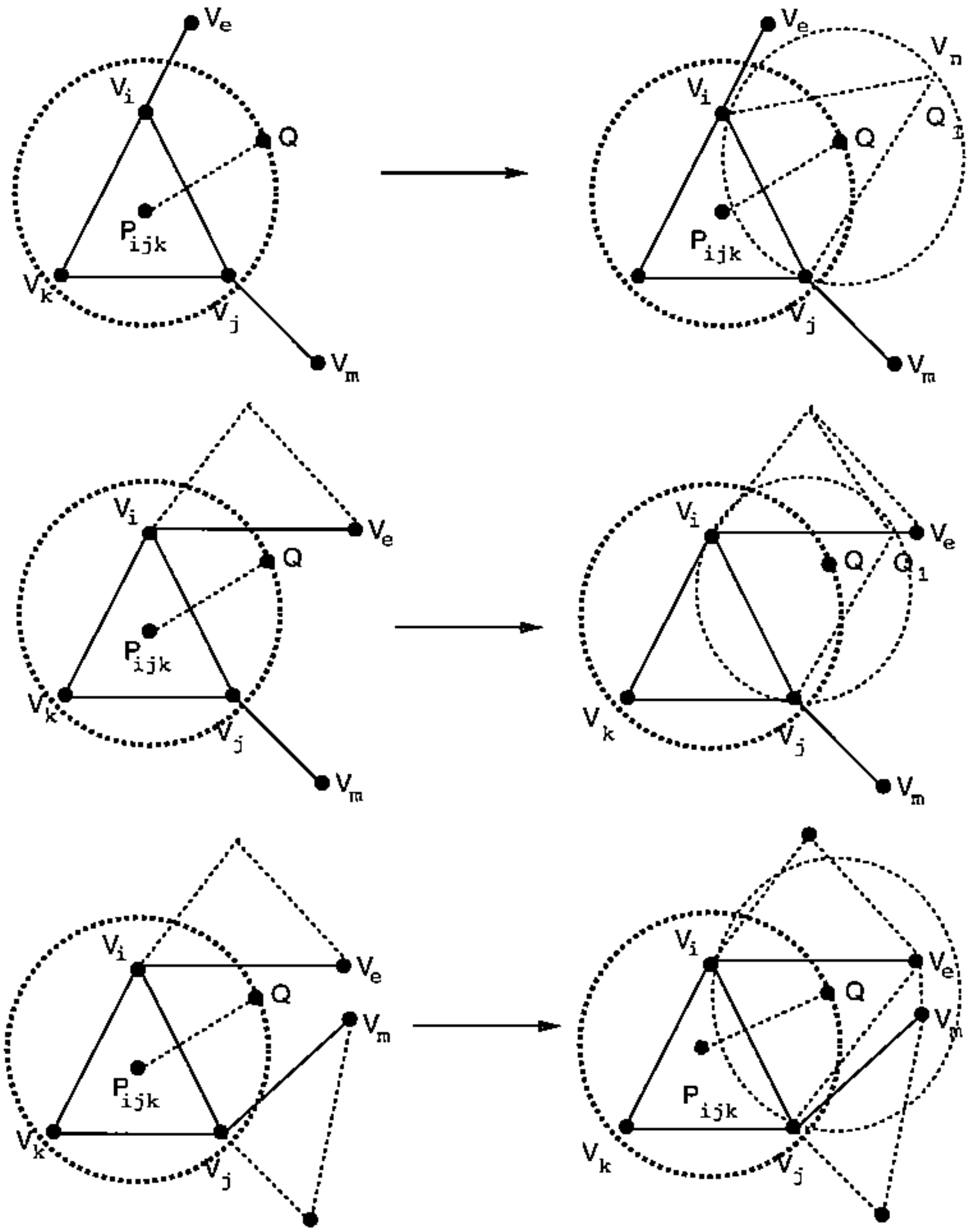

Figure 5: Expansion Steps for the Surface Triangulation

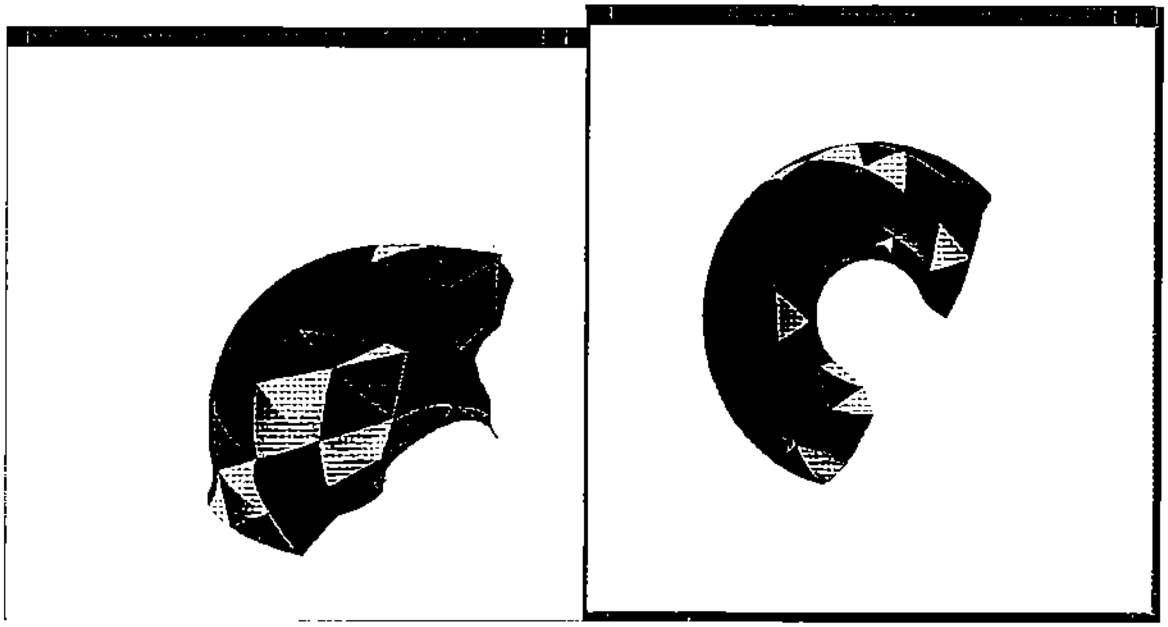

Figure 6: Surface Triangulations of an Implicitly Defined Sphere, Cubic Elbow and a Torus

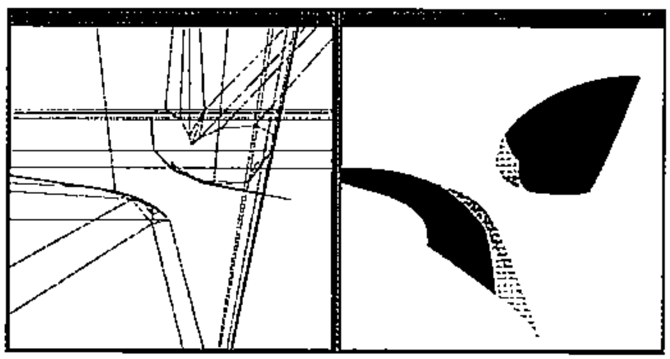

Figure 7: A Quadratic Parametric Surface with Domain Poles

polygonal approximation algorithms to fail. These are ubiquitous problems occurring even among the natural quadrics. See examples shown in Figures 7 and 8.

In geometric design and graphics, where rational Bezier and B-spline surfaces have become popular, the above problems have so far been avoided by a restriction to smooth rational surface patches with denominator polynomials having all positive coefficients [32, 58] (i.e. no real poles or real base points). Sophisticated but unsuspecting triangulation techniques which accept arbitrary rational parametric input (e.g. those implemented in *Maple V*, *Mathematica*, *Macsyma*) produce completely unintelligible results. Our second algorithm provides a complete and general solution to this problem.

We first illustrate the topological problems that arise if one naively mapped a triangulation from the (s,t) domain to the surface in (x,y,z) space, using the rational parametric equations.

1. [Finite Parameter Range] To fully cover the parametric curve or surface, one must allow the parameters to somehow range over the entire parametric domain, which is infinite. For example, the unit sphere $f(x,y,z) = x^2 + y^2 + z^2 - 1 = 0$ has the standard rational parametric representation ($x = \frac{2s}{1+s^2+t^2}, y =$

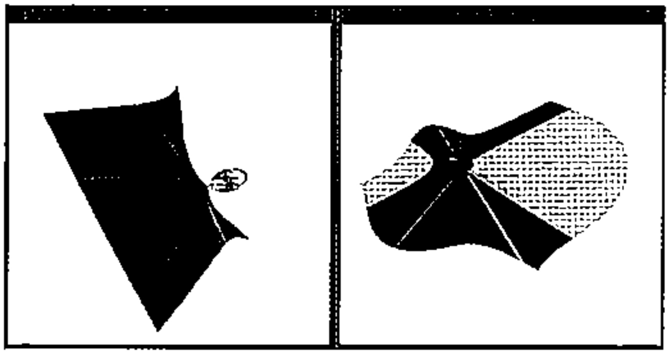

Figure 8: A Cubic Parametric Surface with Seam Curves Due to Base Points

$\frac{2t}{1+s^2+t^2}, z = \frac{1-s^2-t^2}{1+s^2+t^2}$) In this parameterization the point $(0, 0, -1)$ can only be reached by the parameter values $s = t = \infty$.

2. [Poles] Even when restricting the surface to a bounded real part of the parametric domain, the rational functions describing the surface may have poles over that domain. A hyperboloid of two sheets, with implicit equation $z^2 + yz + xz - y^2 - xy - x^2 - 1 = 0$, has the parametric representation ($x(s,t) = \frac{4s}{5t^2+6st+5s^2-1}, y(s,t) = \frac{4t}{5t^2+6st+5s^2-1}, z(s,t) = \frac{5t^2+6st-2t+5s^2-2s+1}{5t^2+6st+5s^2-1}$) then problems arise because of the pole curve described by $5t^2 + 6st + 5s^2 - 1 = 0$ in the parameter domain. See Figure 7.

3. [Base Points] The rational parameter functions describing curves and surfaces are generally assumed to be reduced to lowest common denominators, i.e., the numerator and denominator of each rational function are relatively prime. Thus for a curve, there is no parameter value that can cause both numerator and denominator of a rational parameter function to vanish. For surfaces, the situation is different. For the general parametric representation stated earlier, even if f_1, f_2, f_3, f_4 are relatively prime polynomials, it is still possible that there are a finite number of points (a, b) such that $f_1(a,b) = f_2(a,b) = f_3(a,b) = f_4(a,b) = 0$. Each such point is called a *base point* of the parametric surface and is a value for which the parametric mapping is undefined ($\frac{0}{0}$). There may also be base points at infinity in the parameter domain, and the base points can be complex as well as real-valued. Information about base points can be found in books on algebraic geometry such as [64, 67]. Base points are problematic since there is no one surface point for the corresponding domain point. To each base point there actually corresponds a curve on the surface [64], and since there is no parameter value for surface points on such a curve, the entire curve will be missing from the parametric surface. Such a curve is called a *seam curve*. See the right side of Figure 8 which corresponds the cubic parametric surface $x = \frac{t^3-t+s^3-s^2+1}{t^3+s^3+1}, y = \frac{2t^3-t^2-s^2t+2s^3+2}{t^3+s^3+1}, z = \frac{-st-s^3}{t^3+s^3+1}$. Thus for a valid triangulation of a parametric surface, one should also consistently triangulate the gaps caused by the seam curves.

Finite Parameter Range Solution

In [15], the infinite parameter value problem is solved for rational varieties in any dimension using projective linear transformations of the domain. We reproduce without proof the key results, which are necessary for the triangulation algorithm.

Lemma 3.1 *Consider a rational algebraic variety of dimension n in R^m, $n < m$, given by parametric equations*

$$V(\mathrm{s}) = \begin{pmatrix} x_1(s_1, \ldots, s_n) \\ \vdots \\ x_m(s_1, \ldots, s_n) \end{pmatrix}, \qquad s_i \in [-\infty, +\infty]$$

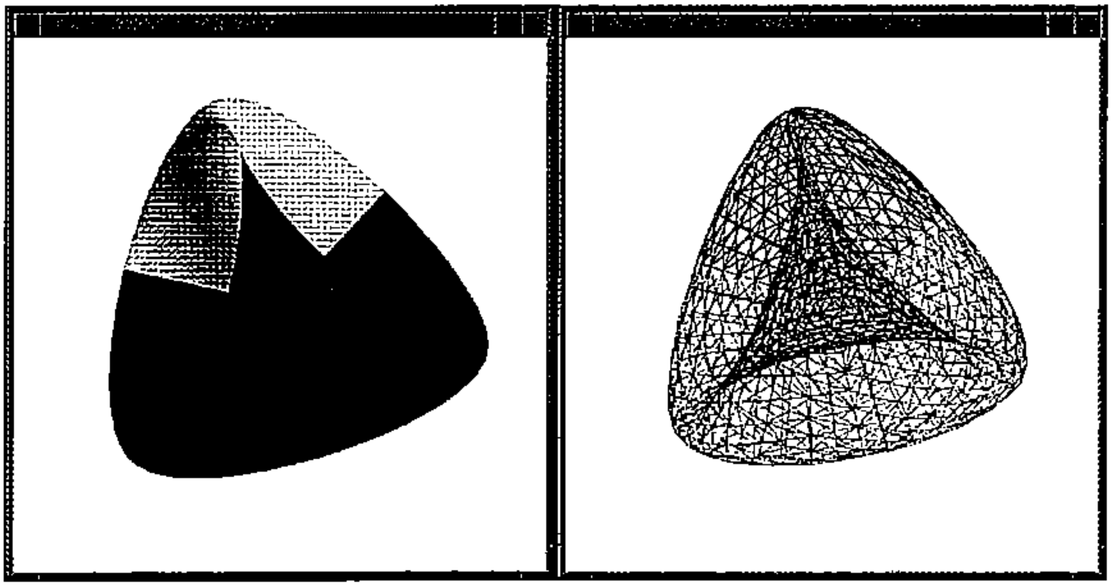

Figure 9: A Complete Triangulation of the Steiner Parametric Surface

Let the 2^n octant cells in the parameter domain R^n be labelled by the tuples $< \sigma_1, \ldots \sigma_n >$ with $\sigma_i \in \{-1, 1\}$. Then the projective reparameterizations $V(\mathrm{t}_{<\sigma_1,\ldots,\sigma_n>})$ given by

$$s_i = \sigma_i \frac{t_i}{1 - t_1 - t_2 - \ldots - t_n}, \qquad i = 1, \ldots, n \tag{4}$$

together map the entire rational variety using only $t_i \geq 0$ such that $0 \leq t_1 + t_2 + \ldots + t_n \leq 1$.

Corollary 3.1 *Rational curves $C(s) = (x_1(s), \ldots, x_m(s))^T$, $s \in [-\infty, +\infty]$ are covered by $C(\frac{t}{1-t})$,$C(\frac{-t}{1-t})$, using only $0 \leq t \leq 1$.*

Corollary 3.2 *Rational surfaces $S(s_1, s_2) = (x_1(s_1, s_2), \ldots, x_m(s_1, s_2))^T$, $s_1, s_2 \in [-\infty, +\infty]$ are covered by*
$S(\frac{t_1}{1-t_1-t_2}, \frac{t_2}{1-t_1-t_2})$, $S(\frac{-t_1}{1-t_1-t_2}, \frac{t_2}{1-t_1-t_2})$,
$S(\frac{-t_1}{1-t_1-t_2}, \frac{-t_2}{1-t_1-t_2})$, $S(\frac{t_1}{1-t_1-t_2}, \frac{-t_2}{1-t_1-t_2})$,
using only $t_i \geq 0 \wedge 0 \leq t_1 + t_2 \leq 1$.

The projective reparameterizations are shown here as fractional affine domain transformations for convenience. In practice, the parametric equations of the rational variety would be homogenized using an additional variable and the numerator and common denominator substituted separately as polynomials, thus avoiding rational function manipulation.

For the Steiner surface ($x = \frac{2st}{1+s^2+t^2}, y = \frac{2s}{1+s^2+t^2}, z = \frac{2t}{1+s^2+t^2}$), and the cubic elbow surface ($x = \frac{4t^2+(s^2+6s+4)t-4s-8}{2t^2-4t+s^2+4s+8}$, y $\frac{4t^2+(-s^2-6s-20)t+2s^2+8s+16}{2t^2-4t+s^2+4s+8}$, $z = \frac{(2s+6)t^2+(-4s-12)t-s^2-4s}{2t^2-4t+s^2+4s+8}$), four different projective reparameterizations yield a complete covering of the rational parametric surface. See Figure 9.

Solution for Domain Poles

The main idea behind the solution is as follows: The (s, t) domain is triangulated in such a way that triangles contain pole points only at their vertices. A domain triangle with a pole at a vertex may map onto an infinite-area surface patch, which may lie partly inside the bounding region. If we determine this to be the case, we binary

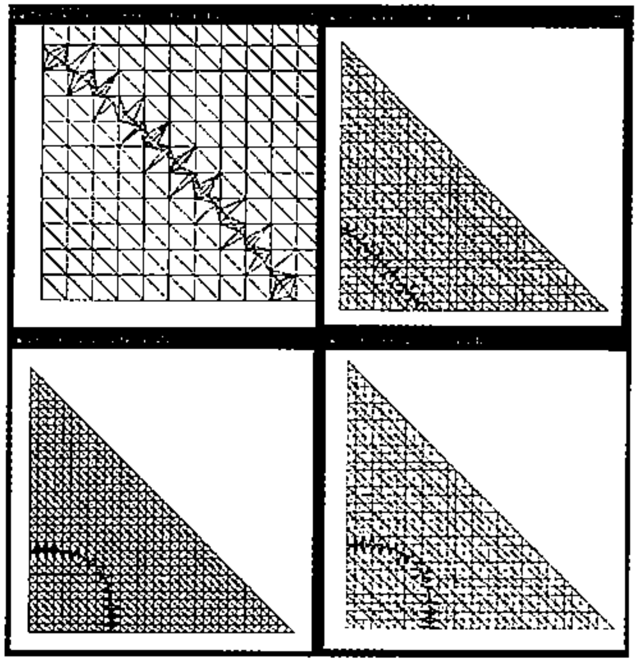

Figure 10: A Domain Triangulation over Unit Simplexes for a Hyperboloid of Two Sheets

search on the edges of the surface triangle for points that intersect the bounding box, clip it with respect to the box and re-triangulate the resulting four or five sided convex polygon on the surface.

The algorithm[14] is as follows.

1. Perform the projective reparameterizations so the entire surface is mapped in four pieces. Perform the next steps for each piece.

2. Generate points on the pole curve that lies inside the unit simplex.

3. Generate points in the rest of the unit simplex according to some scheme. The two kinds of points are distinguished from each other.

4. Compute a triangulation of the points thus generated. If an edge of any such triangle intersects the pole curve, insert the intersection point and recompute the triangulation.

5. Every triangle will then have 0, 1, or 2 pole points. A triangle with 3 pole points is split by inserting a simple point in its interior. See also Figure 10. If a triangle has no pole points, it can be mapped immediately to the surface. Suppose it has one pole point and two regular points. Let the pole point be called p and the regular points q_1, q_2. We denote the surface point corresponding to a point $\mathbf{x}$ as $S(\mathbf{x})$. We assume that $S(\mathrm{p})$ is a point at infinity, which is likely since p is a pole. If $S(q_1), S(q_2)$ both lie outside the bounding region, this triangle will not be mapped. If both lie inside the region, then a binary search is performed along the edges from p to q_1 and p to q_2, for the intersection points $S(\hat{q_1}), S(\hat{q_2})$ with the bounding box. Then mapped surface triangle is thus replaced by a polygon using the two new vertices. By a similar process a a domain triangle with two pole points, and one simple point is either discarded, or the two pole points in the triangle are replaced by regular points whose images are the intersection of the the bounding box and the mapped triangle. Each resulting four or five sided polygon on th surface is convex and easily triangulated.

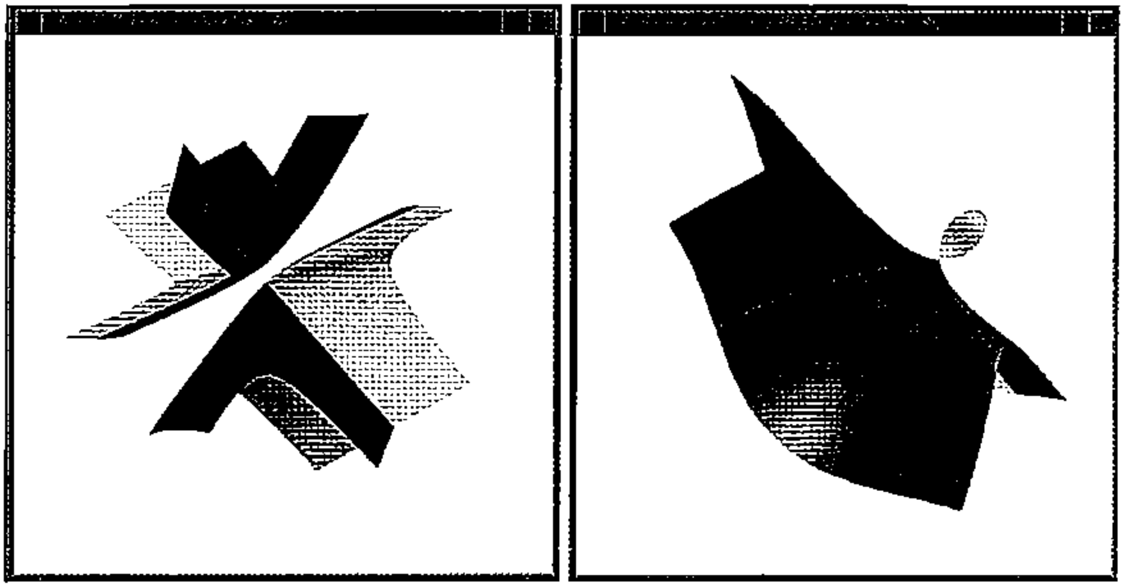

Figure 11: Complete Triangulations and Display of Rational parametric surfaces

Pole curve points with the unit simplex are generated for example by the subdivision method of [37]. In the the second setup, we just generate a constant-size triangular grid on the unit simplex. The grid points are merged with the pole curve points in a special data structure that allows them to be marked as pole or regular points, and an incremental Delaunay triangulation of the entire set of points is constructed [33, 35]. See Figures 10 and ??.

Solution to Base Points

First an important fact about the image of a base point: *Base points blow up to curves on the surface* ([64], Chapter VI, section 2.1, Theorem III, p. 107). Let O be a base point of multiplicity q, and each of the curves $f_1(s,t) = 0, \ldots, f_4(s,t) = 0$ have q distinct tangents at O. Furthermore, let the curves have no common tangents at O. Then the image of the base point O is a curve of degree q on the surface S.

In [16] we show how to compute a parameterization of the seam curve, from the original parameterization and for any base point. For a better correspondence of the surface parameterization to the seam curve parameterization we redefine $X = X(s,t) = f_1(s,t) Y = Y(s,t) = f_2(s,t), Z = Z(s,t) = f_3(s,t), W = W(s,t) = f_4(s,t)$.

Theorem 3.1 *Let (a,b) be an affine base point of multiplicity q. Then for any $m \in \mathcal{R}$, the image of a domain point approaching (a,b) along a line of slope m is given by*

$$(X(m), Y(m), Z(m), W(m)) = \left(\sum_{i=0}^{q} \left(\frac{\partial^q X}{\partial s^{q-i} \partial t^i}(a,b) \right) m^i, \ldots, \sum_{i=0}^{q} \left(\frac{\partial^q W}{\partial s^{q-i} \partial t^i}(a,b) \right) m^i \right) \qquad (5)$$

The points $(X(m), Y(m), Z(m), W(m))$ form a one-dimensional family or curve on the surface S, of degree at most q, called the *seam curve* of the base point (a,b).

Corollary 3.3 *If the curves $X(s,t) = 0, \ldots, W(s,t) = 0$ share t tangent lines at (a,b), then the seam curve $(X(m), Y(m), Z(m), W(m))$ has degree $q-t$. In particular, if $X(s,t) = 0, \ldots, W(s,t) = 0$ have identical tangents at (a,b), then for all $m \in R$ the coordinates $(X(m), \ldots, W(m))$ represent a single point.*

Knowing the parameterization $(X(m), Y(m), Z(m), W(m))$, with parameter m of each real seam curve it is quite straightforward to sample this curve at distinct values of m, and stitch the triangulation together.

4 DATA FITTING

Consider the problem of constructing a C^k mesh of smooth surface patches or *splines* that interpolate or approximate scattered data in $\mathbb{R}^3$. Computations which we would like to optimize by our choice of curve and surface representation include:

- solution requiring a small number of surface patches
- reduction of the fitting problem to solving small linear systems
- low geometric degree of the solution surfaces

There are several possible variants of the problem depending on the nature of the interpolation problem on hand: local versus non-local patch interpolation, splitting v.s. non-splitting of the surface patches per triangulation face, the convexity versus non-convexity of the given triangulation, etc. In each of these cases, the comparison between the implicit versus parametric representation does not yield a clear winner. While the implicit representation yields lower geometric degree solutions (for reasons relating to degrees of freedom and the number of constraints, the parametric surfaces shows a clear advantage when suitable surfaces need to be selected from an infinite family of interpolatory solutions. Straightforward conditions on the parameter domain can yield parametric surface solutions which are free of poles and base points.

The generation of a C^1 mesh of smooth surface patches or *splines* that interpolate or approximate *triangulated space data* is one of the central topics of geometric design. Alfeld [5], Chui [26], Dahmen and Michelli [31] and Hollig [46] summarize much of the history of scattered data fitting and multivariate splines. Prior work on splines have traditionally worked with a given planar triangulation using a polynomial function basis [5, 57, 63]. More recently surface fitting has been considered over closed triangulations in three dimensions using parametric surface patches [22, 20, 24, 34, 38, 42, 45, 47, 51, 53, 54, 55, 59, 65]. Little work has been done on spline bases using implictly defined algebraic surface patches. Sederberg [60, 61] showed how various smooth implicit algebraic surfaces in trivariate Bernstein basis can be manipulated as functions in Bezier control tetrahedra with finite weights. Patrikalakis and Kriezis [52] extended this by considering implicit algebriac surfaces in a tensor product B-spline basis. However the problem of selecting weights or specifying knot sequences for C^1 meshes of implicit algebraic surface patches which fit given spatial data, was left open. Dahmen [29] presented a scheme for constructing C^1 continuous, piecewise quadric surface patches over a data triangulation in space. In his construction each triangular face is split and replaced by six micro quadric triangular patches, similar to the splitting scheme of Powell-Sabin [56]. More on this later. Moore and Warren [50] extend the marching cubes scheme of [48] and compute a C^1 piecewise quadratic approximation (least-squares) to scattered data. They too use a Powell-Sabin like split, however over subcubes.

In paper [13] the authors consider an arbitrary spatial triangulation $\mathcal{T}$ consisting of vertices $\mathbf{p} = (x_i, y_i, z_i)$ in $\mathbb{R}^3$ (or more generally a simplicial polyhedron $\mathcal{P}$ when the triangulation is closed), with possibly "normal" vectors at the vertex points. An algorithm is given to construct a C^1 continuous mesh of low degree real algebraic surface patches S_i over $\mathcal{T}$ or $\mathcal{P}$. The algorithm first converts the given triangulation $\mathcal{T}$ or simplicial polyhedron $\mathcal{P}$ into a curvilinear wireframe (with at most cubic parametric curves) which C^1 interpolates all the vertices, followed by a fleshing of the wireframe with low degree algebraic surface patches. See Figure 12. The technique is completely general and uses a single implicit surface patch of degree at most 7, for each triangular face of $\mathcal{T}$ of $\mathcal{P}$, i.e. no local splitting of triangular faces. Furthermore, the C^1 interpolation scheme is local in that each triangular surface patch has independent degrees of freedom which may be used to provide local shape control. Extra free parameters may be adjusted and the shape of the patch controlled by using weighted least squares approximation from additional points and normals, generated locally for each triangular patch. Similar techniques exist for parametrics [24, 34, 38, 54, 59] however the geometric degree of the solution surfaces tend to be prohibitively high.

In papers [11, 10] we show how to join a collection of cubic A-patches of §2 to form a C^1 smooth surface interpolating scattered data points and respecting the topology of a given surface triangulation T of the points. For this problem, prior approaches have been given by [29] using quadric patches, [30, 39, 40] using cubic patches and [13] using quintic for convex triangulations and degree seven patches for arbitrary surface triangulations T.

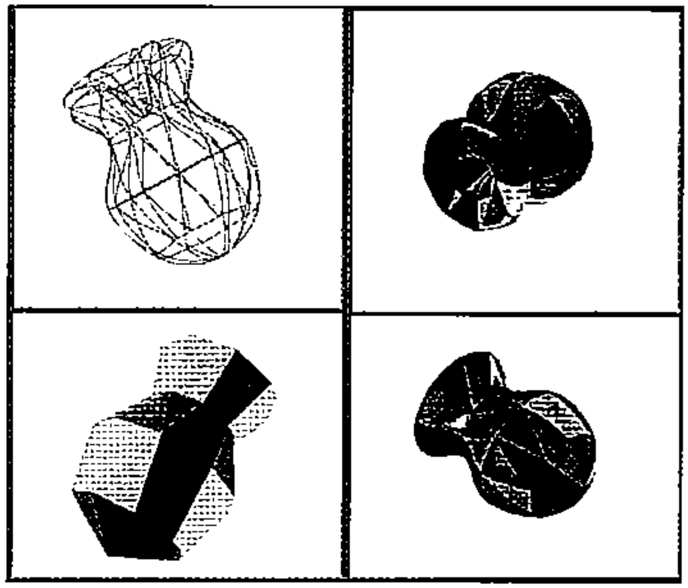

Figure 12: C^1 Implicit Splines over a Spatial Triangulation

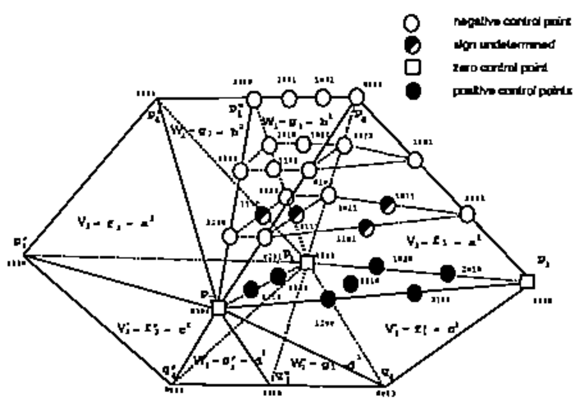

Figure 13: Adjacent Tetrahedra, Cubic Functions and Control Points for two Non-Convex Adjacent Faces

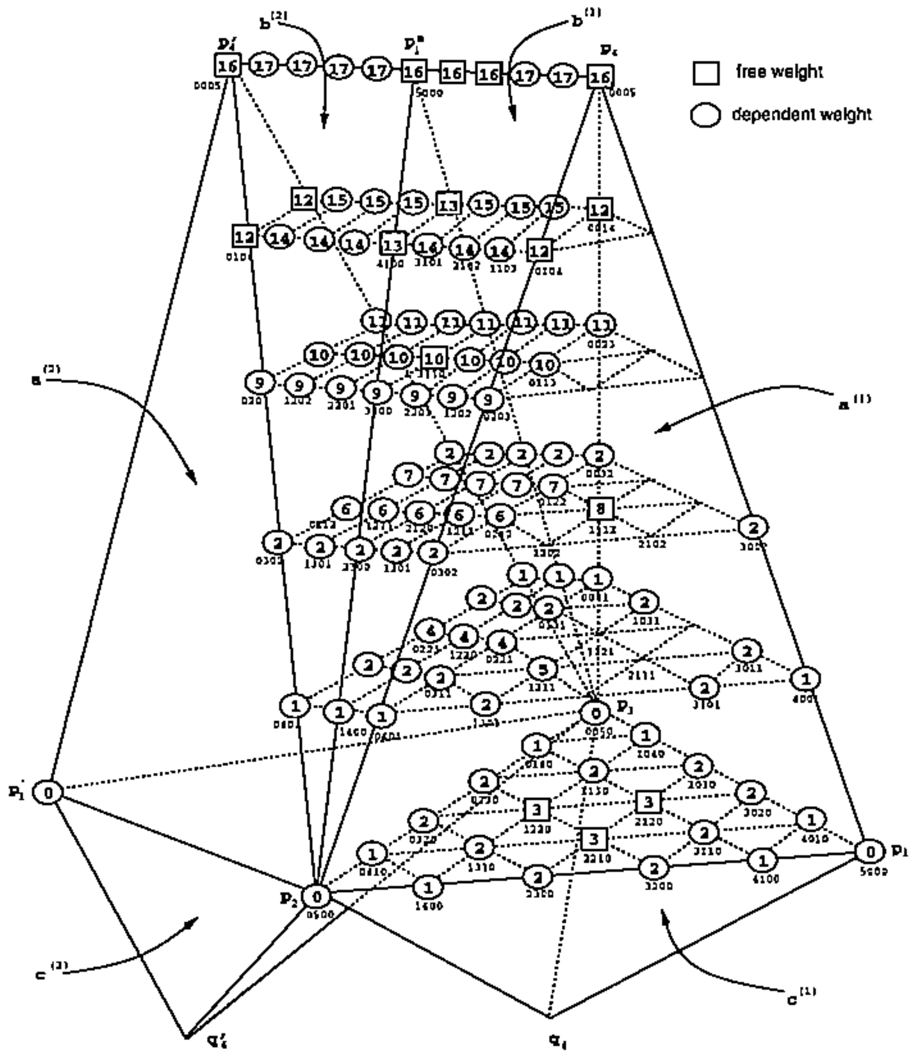

Figure 14: Adjacent Tetrahedra, Quintic Functions and Control Points for two Non-Convex Adjacent Faces

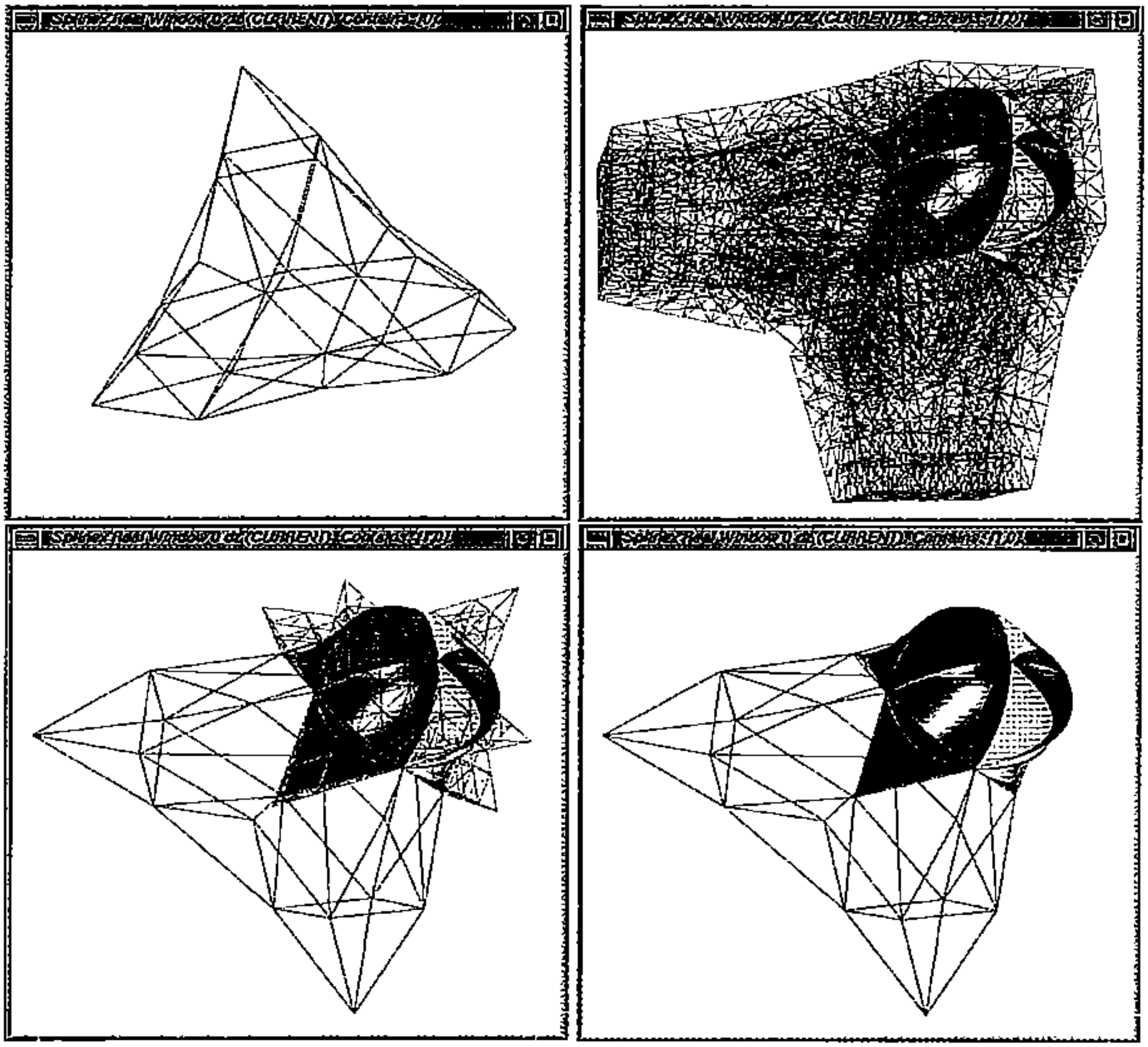

Figure 15: A Surface Triangulation, the Simplicial Hull and some of the interpolatory C^1 Cubic A-Patches

All these papers provide heuristics to overcome the multiple sheeted and singularity problems of implicit patches. In this paper our cubic A-patches are guaranteed to be nonsingular and single sheeted within each tetrahedron.

While the details of the methods of [30] and [40] differ somewhat, they both use the scheme of [29] of building a surrounding simplicial hull (consisting of a series of tetrahedra) of the given triangulation T. Such a simplicial hull is nontrivial to construct for triangulations and neither of the papers [29, 30, 39, 40] enumerate the different exceptional cases (possible even for convex triangulations) nor provide solutions to overcoming them. Paper [11] also uses the same simplicial hull approach but enumerates the exceptional situations and provide strategies for rectifying them. See Figure 15 for an example surface triangulation and its simplicial hull.

In [40], Guo uses a Clough-Tocher split[27] and subdivides each face tetrahedron of the simplicial hull, hence utilizing three patches per face of T. In paper [11], we consider the computed "normals" at the given data points, and distinguish between "convex" and "non-convex" faces and edges of the triangulation. We use a single cubic A-patch per face of T except for the following two special cases. For a non-convex face, if additionally the three inner products of the face normal and its three adjacent face normals have different signs, then in this case one needs to subdivide the face using a single Clough-Tocher split, yielding C^1 continuity with the help of three cubic

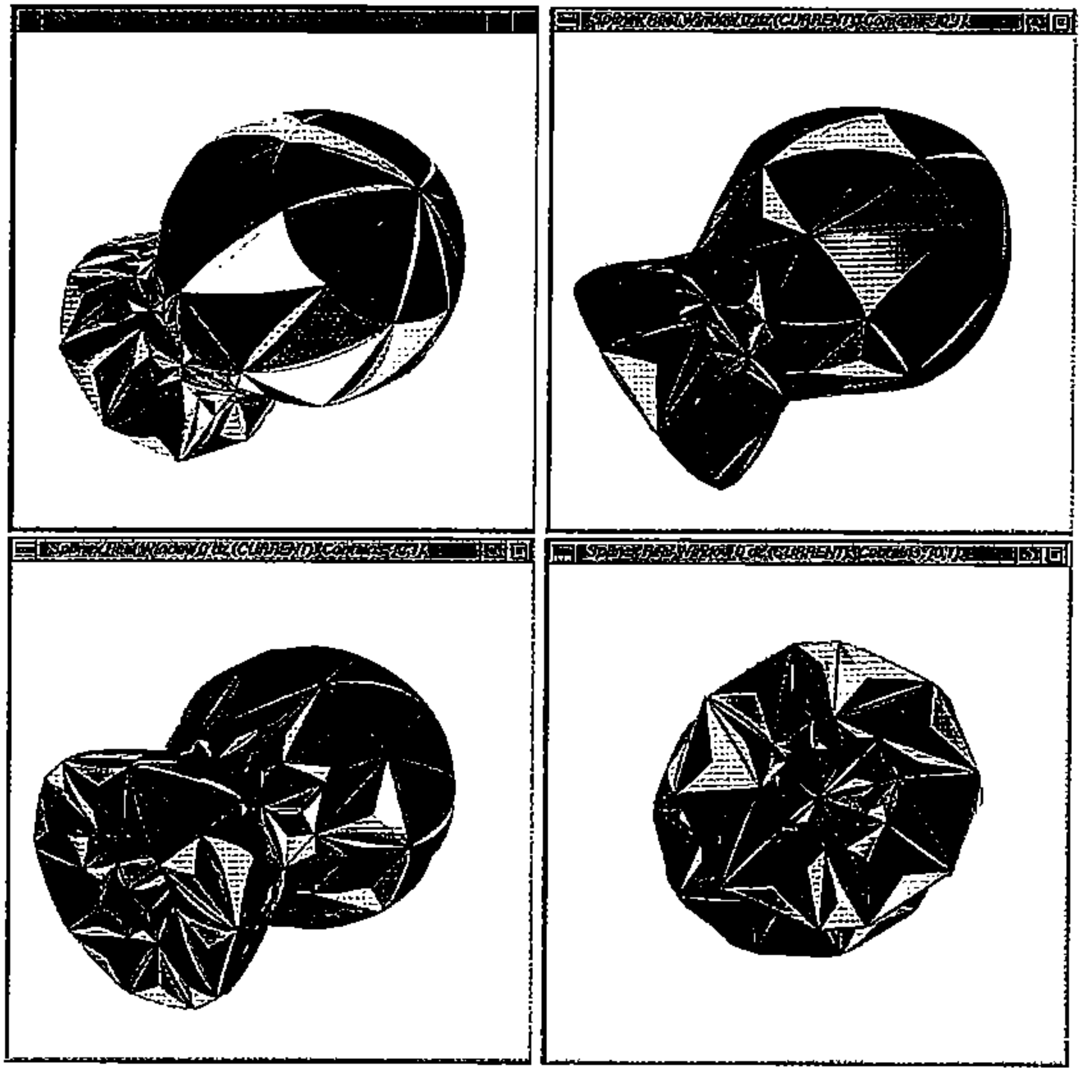

Figure 16: The Complete Smoothing of the Surface Triangulation using C^1 Cubic A-Patches

A-patches for that face. Furthermore for coplanar adjacent faces of T, we show that the C^1 conditions cannot be met using a single cubic A-patch for each face. Hence for this case we again use Clough-Tocher splits for the pair of coplanar faces yielding C^1 continuity with the help of three cubic A-patches per face. See Figures 15,16 for examples of the C^1 interpolation of polyhedra.

The C^1 interpolation schemes of [11, 29, 30, 40, 41] all build an outside simplicial hull (consisting of a series of edge and face tetrahedra) containing the given polyhedron $\mathcal{P}$. As mentioned before, such a simplicial hull is nontrivial to construct for arbitrary $\mathcal{P}$ (even convex $\mathcal{P}$ with sharp corners) and can give rise to several exceptional situations and degeneracies (co-planarity, hull self-intersection, etc). In [12] a new corner-cutting, inner simplicial hull construction is presented and can handle all convex $\mathcal{P}$ and also arbitrary polyhedra with non-convex faces. This new simplicial hull scheme is the three dimensional generalization of the two-dimensional corner-cutting scheme used to construct C^k continuous bivariate A-splines [18]. Using this new hull construction technique paper [12] presents efficient algorithms to construct both a C^1 smooth mesh with cubic A-patches and C^2 smooth mesh with cubic and quintic A-patches to approximate a given polyhedron $\mathcal{P}$ in three dimensions.

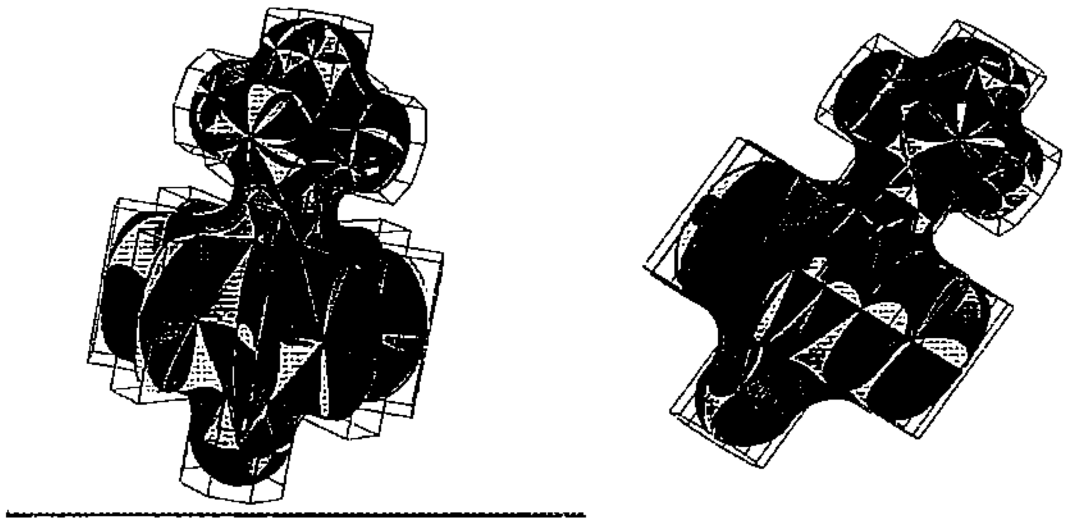

(a) (b)

Figure 17: C^1 and C^2 Smooth Approximations

For the construction of smooth patch complexes within the simplicial hull built on two adjacent triangles(see Figure 13 for C^1 and Figure 14 for C^2.

See also Figures 17 and 18 for examples of the C^1 and C^2 approximation of polyhedra and their shape modification.

5 QUICKTIME MOVIES

The CDROM includes two QuickTime movies showing algorithmic animations of :

1. Shows algorithmic animation of the C^1 interpolatory cubic A-patch data fitting scheme[11] discussed in the previous section. The patch computations and display are done using a network of workstations, with individual patch computations done on separate machines.
2. Shows algorithmic animation of C^1 smooth surface reconstructions from unorganized data points[9]. In this movie one has used tensor-product A-patches (defined over cuboids) as opposed to the triangular A-patches of the first movie.

Acknowledgement: Implementations of the above algorithms (for parametric and implicit surface patches), the figures and the two QuickTime movies shown were all accomplished in SHASTRA, a distributed and collaborative (multi-user, multi-workstation) free-form geometric design and visualization environment developed by the author at Purdue University. Information on SHASTRA software availability can be obtained from the author or via anonymous ftp from ftp.cs.purdue.edu:pub/shastra/ and via the world wide web hypertext program Mosaic from http://www.cs.purdue.edu/research/shastra/shastra.html.

References

[1] S. Abhyankar and C. Bajaj. Automatic Rational Parameterization of Curves and Surfaces I: Conics and Conicoids. *Computer Aided Design*, 19(1):11–14, 1987.

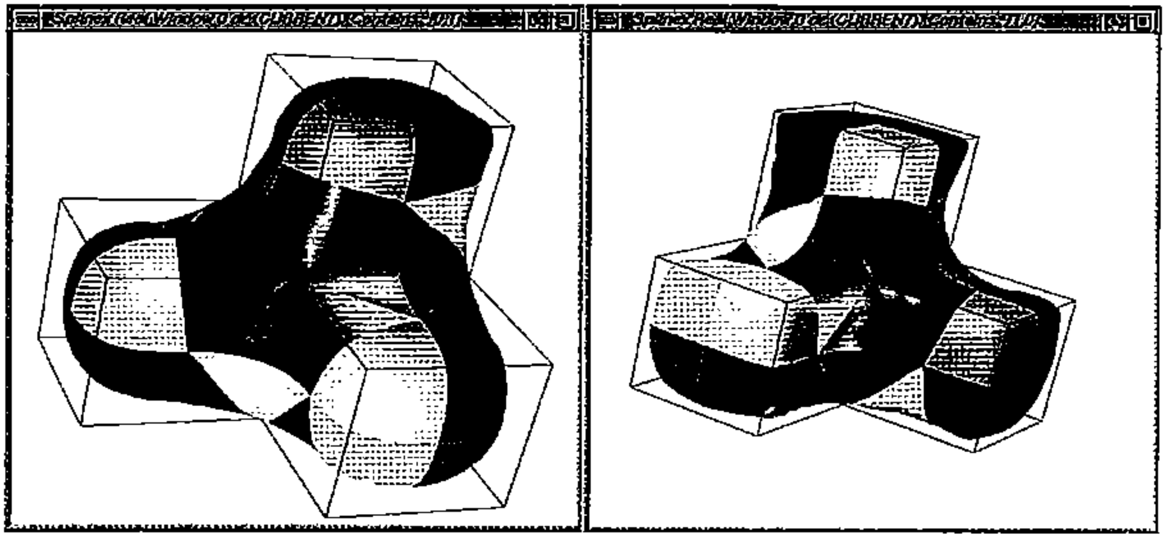

Figure 18: Shape Control of Smooth Approximations of a Polyhedron

[2] S. Abhyankar and C. Bajaj. Automatic Rational Parameterization of Curves and Surfaces II: Cubics and Cubicoids. *Computer Aided Design*, 19(9):499–502, 1987.

[3] S. Abhyankar and C. Bajaj. Automatic Rational Parameterization of Curves and Surfaces III: Algebraic Plane Curves. *Computer Aided Geometric Design*, 5(1):309–321, 1988.

[4] S. Abhyankar and C. Bajaj. Automatic Rational Parameterization of Curves and Surfaces IV: Algebraic Space Curves. *ACM Transactions on Graphics*, 8(4):324 – 333, 1989.

[5] P. Alfeld. Scattered Data Interpolation in Three or More Variables. In T. Lyche and L. Schumaker, editors, *Mathematical Methods in Computer Aided Geometric Design*, pages 1–34. Academic Press, 1989.

[6] Allgower, E., and Gnutzmann, S.,. Simplicial Pivoting for Mesh Generation of Implicitly Defined Surfaces. *Computer Aided Geomtric Design*, pages 305–325, 1991.

[7] C. Bajaj. Geometric modeling with algebraic surfaces. In D. Handscomb, editor, *The Mathematics of Surfaces III*, pages 3–48. Oxford Univ. Press, 1988.

[8] C. Bajaj. The Emergence of Algebraic Curves and Surfaces in Geometric Design. In R. Martin, editor, Directions in Geometric Computing, pages 1 – 29. Information Geometers Press, 1993.

[9] C. Bajaj, F. Bernardini, and G. Xu. *Reconstruction of Surfaces and Surfaces-on-Surfaces from Unorganized Weighted Points.* Computer Science Technical Report, CS-94-001, Purdue University, 1994.

[10] C. Bajaj, J. Chen, and G. Xu. *Modeling with Cubic A-Patches.* Computer Science Technical Report, CSD-TR-93-02, Purdue University, 1993.

[11] C. Bajaj, J. Chen, and G. Xu. Free form surface design with a-patches. In *Proceedings of Graphics Interface'94*, pages x–y, Banff, Canada., 1994.

[12] C. Bajaj, J. Chen, and G. Xu. *Smooth Low Degree Approximations of Polyhedra.* Computer Science Technical Report, CSD-TR-94-002, Purdue University, 1994.

[13] C. Bajaj and I. Ihm. C^1 Smoothing of Polyhedra with Implicit Algebraic Splines. *SIGGRAPH'92, Computer Graphics*, 26(2):79–88, 1992.

[14] C. Bajaj and A. Royappa. The Robust Display of Arbitrary Rational Parametric Surfaces. In *Curves and Surfaces in Computer Vision and Graphics III*, pages 70 – 80, Boston, MA, 1992.

[15] C. Bajaj and A. Royappa. *Finite Representation of Parametric Curves and Surfaces.* In *Proc. of IFIP TC 5/WG 5.10 II Conference on Geometric Modeling in Computer Graphics*, pages x–y, Genova, Italy, 1993.

[16] C. Bajaj and A. Royappa. *Topologically Correct Approximations of Arbitrary Rational Parametric Surfaces.* Computer Science Technical Report, CAPO 93-06, Purdue University, 1993.

[17] C. Bajaj and G. Xu. *Piecewise Rational Approximation of Real Algebraic Curves.* Computer Science Technical Report, CAPO-91-19, Purdue University, 1991.

[18] C. Bajaj and G. Xu. *A-Splines: Local Interpolation and Approximation using C^k-Continuous Piecewise Real Algebraic Curves.* Computer Science Technical Report, CAPO-92-44, Purdue University, 1992.

[19] C. Bajaj and G. Xu. *NURBS Approximation of Surface-Surface Intersection Curves.* Computer Science Technical Report, CAPO-92-17, Purdue University, 1992.

[20] C. Bajaj and G. Xu. *Piecewise Rational Approximation of Real Algebraic Surfaces.* Computer Science Technical Report, CAPO 93-21, Purdue University, 1993.

[21] C. Bajaj and G. Xu. Rational spline approximations of real algebraic curves and surfaces. In H.P. Dikshit and C. Michelli, editors, Advances in Computational Mathematics, pages x–x. World Scientific Publishing Co., 1994.

[22] Beeker, E. Smoothing of Shapes Designed with Free Form Surfaces. *Computer Aided Design*, 18(4):224–232, 1986.

[23] Bloomenthal, J. Polygonization of Implicit Surfaces. *Computer Aided Geometric Design*, 5:341–355, 1988.

[24] Chiyokura, H., and Kimura, F. Design of Solids with Free-form Surfaces. *Computer Graphics*, 17(3):289–298, 1983.

[25] Chuang, J.,. *Surface Approximations in Geomtric Modeling.* PhD thesis, Computer Science, Purdue University, 1990.

[26] Chui, C. *Multivariate Splines.* Regional Conference Series in Applied Mathematics, 1988.

[27] R. Clough and J. Tocher. Finite Element Stiffness Matrices for Analysis of Plates In Bending. In Proceedings of Conference on Matric Methods in Structural Analysis, 1965.

[28] G. Collins. Quantifier Elimination for Real Closed Fields: A Guide to the Literature, in *computer algebra, symbolic and algebraic computation*, 1983.

[29] W. Dahmen. Smooth piecewise quadratic surfaces. In T. Lyche and L. Schumaker, editors, *Mathematical Methods in Computer Aided Geometric Design*, pages 181–193. Academic Press, Boston, 1989.

[30] W. Dahmen and T-M. Thamm-Schaar. Cubicoids: modeling and visualization. *Computer Aided Geometric Design*, 10:93–108, 1993.

[31] Dahmen, W. and Micchelli, C. Recent Progress in Multivariate Splines. In L. Schumaker C. Chui and J. Word, editors, *Approximation Theory IV*, pages 27–121. Academic Press, 1983.

[32] DeRose, T. Rational Bezier Curves and Surfaces on Projective Domains. In G. Farin, editor, *NURBS for Curve and Surface Design*, pages 1–14. SIAM, 1991.

[33] H. Edelsbrunner. Algorithms in Combinatorial Geometry. Springer Verlag, 1987.

[34] G. Farin. Triangular Bernstein-Bézier patches. *Computer Aided Geometric Design*, 3:83–127, 1986.

[35] Fortune S.,. Numerical Stability of Algorithms for 2D Delaunay Triangulations. In Proc. of the 8th ACM Symposium on Computational Geometry, pages 83–92, 1989.

[36] Garrity, T., and Warren, J. Geometric continuity. *Computer Aided Geometric Design*, 8:51–65, 1991.

[37] Geisow, A.,. *Surface Interrogations.* PhD thesis, University of Anglia, School of computing Studies and Accountancy, 1983.

[38] Gregory, J., and Charrot, P. A C^1 Triangular Interpolation Patch for Computer Aided Geometric Design. *Computer Graphics and Image Processing*, 13:80–87, 1980.

[39] B. Guo. *Modeling Arbitrary Smooth Objects with Algebraic Surfaces.* PhD thesis, Computer Science, Cornell University, 1991.

[40] B. Guo. Surface generation using implicit cubics. In N.M. Patrikalakis, editor, *Scientific Visualizaton of Physical Phenomena*, pages 485–530. Springer-Verlag,Tokyo, 1991.

[41] B. Guo. Non-splitting Macro Patches for Implicit Cubic Spline Surfaces. *Computer Graphics Forum*, 12(3):434 – 445, 1993.

[42] Hagen, H., and Pottmann, H. Curvature Continuous Triangular Interpolants. *Mathematical Methods in Computer Aided Geometric Design*, pages 373–384, 1989.

[43] Hall, M., and Warren, J. Adaptive Polygonalization of Implicitly Defined Surfaces. *IEEE Computer Graphics and Applications*, pages 33–42, 1990.

[44] P. Henrici. *Applied and Computational Complex Analysis*, 1988.

[45] Herron, G. Smooth Closed Surfaces with Discrete Triangular Interpolants. *Computer Aided Geometric Design*, 2(4):297–306, 1985.

[46] Hollig, K. Multivariate Splines. *SIAM J. on Numerical Analysis*, 19:1013–1031, 1982.

[47] Liu, D., and Hoschek, J. GC^1 Continuity Conditions Between Adjacent Rectangular and Triangular Bezier Surface Patches. *Computer Aided Design*, 21:194–200, 1989.

[48] Lorensen, W., and Cline, H. Marching Cubes: A High Resolution 3D Surface Construction Algorithm. *Computer Graphics*, 21:163–169, 1987.

[49] Micchelli, C., and Prautzsch, H.,. Computing Surfaces Invariant under Subdivision. *Computer Aided Geometric Design*, 4:321–328, 1987.

[50] D. Moore and J. Warren. Approximation of dense scattered data using algebraic surfaces. In *Proc. of the 24th Hawaii Intl. Conference on System Sciences*, pages 681–690, Kauai, Hawaii, 1991.

[51] Nielson, G. A Transfinite Visually Continuous Triangular Interpolant. In G. Farin, editor, *Geometric Modeling Applications and New Trends.* SIAM, 1986.

[52] Patrikalakis, N., and Kriezis, G. Representation of Piecewise Continuous Algebraic Surfaces in Terms of B-splines. *The Visual Computer*, 5(6):360–374, Dec. 1989.

[53] Peters, J. Local Cubic and BiCubic C^1 Surface Interpolation with Linearly Varying Boundary Normal. *Computer Aided Geometric Design*, 7:499–516, 1990.

[54] Peters, J. Smooth Interpolation of a Mesh of Curves. *Constructive Approximation*, 7:221–246, 1991.

[55] Piper, B. Visually Smooth Interpolation with Triangular Bezier Patches. In G. Farin, editor, *Geometric Modeling: Algorithms and New Trends.* SIAM, 1987.

[56] Powell, M., and Sabin, M. Piecewise Quadratic Approximations on Triangles. *ACM Trans. on Math. Software,* 3:316–325, 1977.

[57] Ramshaw, L. Beziers and B-splines as Multiaffine Maps. In *Theoretical Foundations of Computer Graphics and CAD.* Springer Verlag, 1988.

[58] Rockwood, A., Heaton, K., and Davis, T. Real-Time Rendering of Trimmed Surfaces. *Computer Graphics,* 23(3):107–116, 1989.

[59] R. Sarraga. G^1 interpolation of generally unrestricted cubic Bézier curves. *Computer Aided Geometric Design,* 4:23–39, 1987.

[60] T.W. Sederberg. Piecewise algebraic surface patches. *Computer Aided Geometric Design,* 2(1-3):53–59, 1985.

[61] T.W. Sederberg. Techniques for cubic algebraic surfaces, tutorial part ii. *IEEE Computer Graphics and Applications,* 10(5):12–21, Sept. 1990.

[62] Sederberg, T., and J. Snively, J.,. Parameterization of Cubic Algebraic Surfaces. In Oxford University Press R. Martin, editor, *The Mathematics of Surfaces II,* 1987.

[63] Seidel, H-P. A New Multiaffine Approach to B-splines. *Computer Aided Geometric Design,* 6:23–32, 1989.

[64] Semple, J., and Roth, L. *Introduction to Algebraic Geometry.* Oxford University Press, Oxford, U.K., 1949.

[65] Shirman, L., and Sequin, C. Local Surface Interpolation with Bezier Patches. *Computer Aided Geometric Design,* 4:279–295, 1987.

[66] Walker, R. *Algebraic Curves.* Springer Verlag, 1950.

[67] Zariski, O. *Algebraic Surfaces.* Ergebnisse der Mathematik und ihre Grenzgebiete 4, 1935.

[68] Zariski, O., and Samuel, P. *Commutative Algebra (Vol. I, II).* Springer Verlag, 1958.